ACS SyntheticBiology

pubs.acs.org/synthbio

Research Article

A Golden-Gate Based Cloning Toolkit to Build Violacein Pathway Libraries in *Yarrowia lipolytica*

Yingjia Tong, Jingwen Zhou, Liang Zhang,* and Peng Xu*

Cite This: *ACS Synth. Biol.* 2021, 10, 115−124

Read Online

ACCESS | Metrics & More | Article Recommendations | Supporting Information

ABSTRACT: Violacein is a naturally occurring anticancer therapeutic compound with deep purple color. In this work, we harnessed the modular and combinatorial feature of a Golden Gate assembly method to construct a library of violacein producing strains in the oleaginous yeast *Yarrowia lipolytica*, where each gene in the violacein pathway was controlled by three different promoters with varying transcriptional strength. After optimizing the linker sequence and the Golden Gate reaction, we achieved high transformation efficiency and obtained a panel of representative *Y. lipolytica* recombinant strains. By evaluating the gene expression profile of 21 yeast strains, we obtained three colorful compounds in the violacein pathway: green (proviolacein), purple (violacein), and pink (deoxyviolacein). Our results indicated that strong expression of *VioB*, *VioC*, and *VioD* favors violacein production with minimal byproduct deoxyvioalcein in *Y. lipolytica*, and high deoxyviolacein production was found strongly associated with the weak expression of *VioD*. By further optimizing the carbon to nitrogen ratio and cultivation pH, the maximum violacein reached 70.04 mg/L with 5.28 mg/L of deoxyviolacein in shake flasks. Taken together, the development of Golden Gate cloning protocols to build combinatorial pathway libraries, and the optimization of culture conditions set a new stage for accessing the violacein pathway intermediates and engineering violacein production in *Y. lipolytica*. This work further expands the toolbox to engineering *Y. lipolytica* as an industrially relevant host for plant or marine natural product biosynthesis.

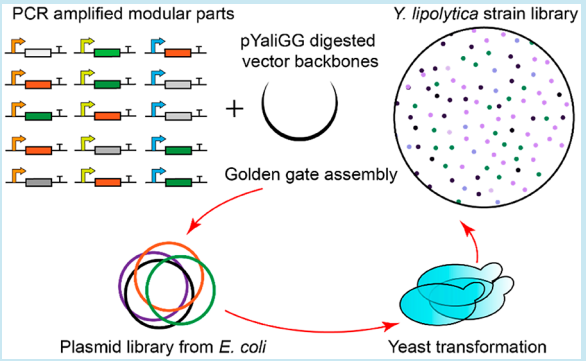

KEYWORDS: *Yarrowia lipolytica, violacein, Golden-Gate cloning, library construction, promoter engineering, fermentation optimization*

INTRODUCTION

Violacein and deoxyviolacein belong to bisindol pigments with deep purple color, which are derived from the tryptophan biosynthetic pathway and naturally produced by a number of marine bacteria, such as *Janthinobacterium lividum*,[1,2] *Chromobacterium violaceum*,[3−5] and *Pseudoalteromonas luteoviolacea*.[6] Clinical trials and biomedical studies indicate both compounds possess strong antibacterial,[3,7] anticancer,[8] antiviral,[9] trypanocidal,[10] and antiprotozoal[11] properties. These characteristics make violacein a superior chemical scaffold and drug candidate for the development of clinically active antimicrobial, antiviral, and chemotherapeutic agents.

The violacein biosynthetic pathway was first discovered by Pemberton et al.[12] in 1991 and was fully characterized by Balibar et al.[13] and Sanchez et al.[14] in 2006. Branched from the L-tryptophan pathway, the violacein biosynthetic pathway involves five steps, encoded by *vio*A, *vio*B, *vio*C, *vio*D, and *vio*E,[15] which were organized in an operon form containing all five genes. Two molecules of L-tryptophan are oxidatively condensed by *vio*A and *vio*B to form indole-3-pyruvic acid (IPA). Then, IPA is decarboxylated to form protodeoxyviolaceinic acid via *vio*E. Subsequently, protodeoxyviolaceinate is oxidized to violacein by *vio*D and *vio*C (Figure 1). Without involving the first reduction step of *vio*D, deoxyviolacein is formed as the major byproduct.[15−17]

At present, most of the reported violacein-producing hosts are Gram-negative bacteria with human pathogenicity. For example, both *C. violaceum*[3−5] and *J. lividum*[1,2] have been related with serious skin infection in immune-compromised people, and both strains have been classified as biosafety level II bacteria. Although the native hosts demonstrate some advantage to produce violacein, their pathogenicity significantly limited their industrial application. *Yarrowia lipolytica* has been considered to be nonpathogenic and has been classified as 'generally regarded as safe' (GRAS) by the US Food and Drug Administration (FDA).[18] Both *Y. lipolytica* and *C. violacein* were isolated from the marine environment with high GC content (up to 65% in the coding sequence). We argue that *Y. lipolytica* might be engineered as a novel platform

Received: September 9, 2020
Published: January 5, 2021

https://dx.doi.org/10.1021/acssynbio.0c00469
ACS Synth. Biol. 2021, 10, 115−124

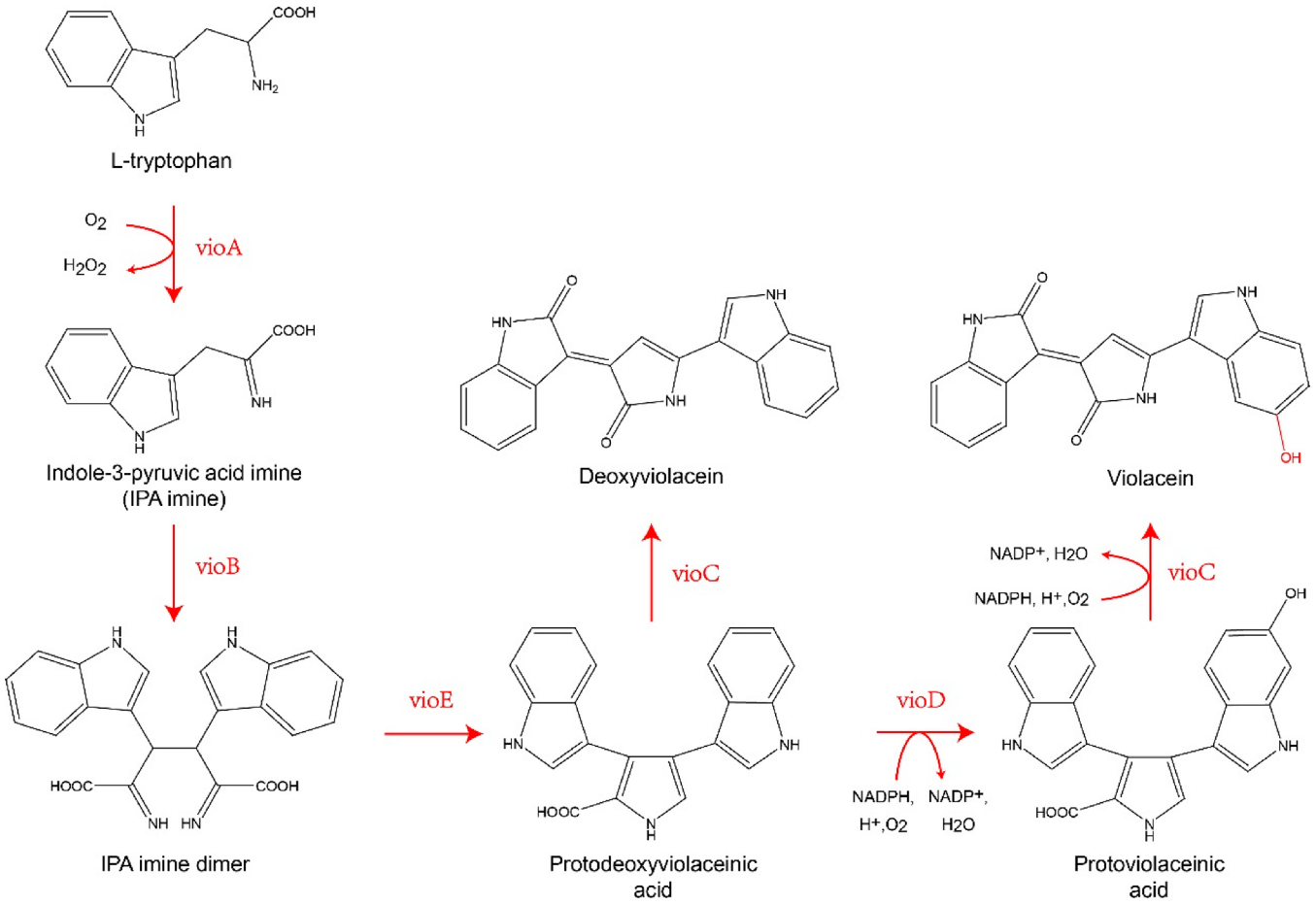

Figure 1. Biosynthetic pathway of violacein: VioA, L-tryptophan oxidase; VioB, *N*-[2-(carboxylatoamino)-1,2-bis(1*H*-indol-3-yl)ethyl]carbamate synthase; VioC, violacein synthase; VioD, protoviolaceinate synthase; VioE, protodeoxyviolaceinate synthase.

for violacein production due to its GRAS status. Different from *Saccharomyces cerevisiae*, *Y. lipolytica* lacks Crabtree effects and does not produce ethanol when carbohydrates are oversupplied in the media.[19] *Y. lipolytica* has been reported to grow on a wide range of inexpensive raw materials,[20] including glucose,[21] glycerol,[22] xylose,[20,23] volatile fatty acids,[24−26] alcohols,[24] and wax alkanes.[27]

Over the past few years, multiple DNA modular assembly platforms have been developed.[28,29] Among them, Golden Gate assembly, which adopts the type IIs restriction enzymes that cut outside of their recognition sequence and generate 4-bp sticky ends, has been considered as one of the most promising methods.[30] It avoids some tedious procedures of traditional cloning such as primer design, PCR amplification, and gel purification. Different from the Gibson assembly method, it does not need overlapping sequences, and only needs type IIs restriction enzyme sites and the four base pair linkages.[31,32] Designing these 4-bp sticky end bases allows for directional and seamless assembly of multiple fragments at one time, and is critical to the successful and efficient assembly of large biosynthetic gene clusters.[33] Golden Gate cloning also allows for combinatorial assembly of multiple functional bioparts, including promoters, ribosomal binding sites, protein coding sequences and terminators, and so on. One can easily shuffle the order of the operon structure and permutate the coding sequence to explore a wide range of gene expression space if multiple regulatory elements are used. Recently, Golden Gate based cloning has been used to express glycerol kinase for conversion of glycerol to erythritol and citric acid in *Y. lipolytica*;[34] a set of modular Golden Gate cloning vectors were also built for rapid construction of the carotenoids pathway[30] and a 3-step xylose utilization pathway in *Y. lipolytica*.[35] However, none of the mentioned work has demonstrated the construction of multiple-gene pathway libraries as well as tuning gene expression with varying promoter strengths in *Y. lipolytica*.

In this work, three different endogenous promoters of *Y. lipolytica*, with high, medium, and low transcriptional activity, were used to control the transcriptional strength of the five genes encoding the violacein pathway, aiming to fine-tune the gene expression and improve the pathway efficiency. To enable rapid and efficient assembly, the Golden Gate assembly method was used for library construction. We have optimized the 4-bp overhangs linkers to improve the assembly efficiency. Upon characterizing the strains from a representative collection of library, we found that the optimal violacein production in *Y. lipolytica* requires strong expression for all the five genes. Thus, we reconstructed the violacein pathway by placing the strongest TEF promoter upstream of all the five genes in the violacein pathway, generating strain *Y. lipolytica* OV1 that yielded 38.68 mg/L violacein and 4.02 mg/L deoxyviolacein in shake flasks. Furthermore, we optimized the yeast cultivation conditions, including carbon to nitrogen ratio (C/N) and pH conditions. The maximum violacein and deoxyviolacein production reached 70.04 mg/L and 5.28 mg/L in shake flasks, respectively, with a C/N molar ratio at 60 and

https://dx.doi.org/10.1021/acssynbio.0c00469
ACS Synth. Biol. 2021, 10, 115−124

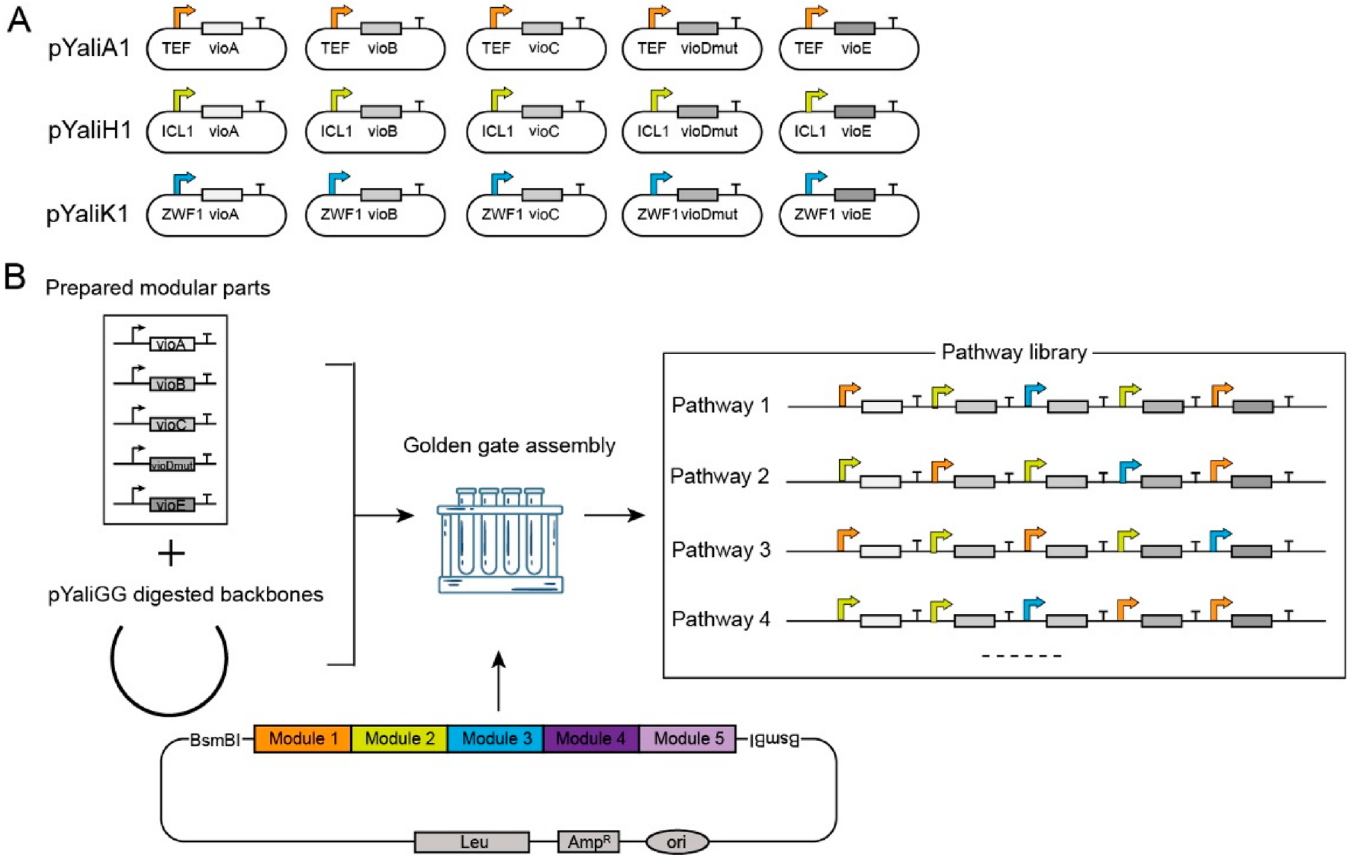

Figure 2. Illustration of engineering strategies with Golden Gate assembly: (A) 15 plasmids that used as modular parts in Golden Gate assembly; (B) overall workflow of Golden Gate assembly used in this work.

the addition of 10 g/L $CaCO_3$ to control the medium pH. Taken together, the development of the Golden Gate-based library construction method and the optimization of culture conditions set a baseline for engineering violacein production in *Y. lipolytica*. The reported work provides a basis for us to engineer efficient and scalable violacein production from the novel host oleaginous yeast species.

RESULTS AND DISCUSSION

Preparing Modular Parts for Golden Gate Assembly. Balancing gene expression within a predefined biosynthetic gene cluster is a common practice to maximize the catalytic efficiency, minimize the metabolic burden, and improve the production and yield.[36] However, when the number of genes and regulatory elements such as promoters or RBSs are large, this method usually represents tedious and time-consuming steps to build the library and screen the best performing strains. In terms of rapid library construction, Golden Gate assembly, first discovered in 1996, is considered as one of the most promising methods because digestion and ligation can be done in a one-pot 30 min reaction.[37,38] To build a violacein-producing library with *Y. lipolytica* as host, the expression of the five genes, including *vio*A, *vio*B, *vio*C, *vio*D, and *vio*E (from *Chromobacterium violaceum*), were placed under the control of three promoters with varying transcriptional strength. We have selected three endogenous promoters from *Y. lipolytica*, namely, the TEF promoter, the ICL1 promoter, and the ZWF1 promoter, with high, medium, and low transcriptional activity, according to our previous studies.[39]

To successfully assemble the five genes and three promoters through the Golden Gate assembly method, we first modified our YaliBrick vectors by removing the internal *Bsm*BI restriction enzyme site on the vector backbone, yielding our Golden Gate vector pYaliGG. Next, the internal BsmBI site within the gene *vio*D underwent silence mutation to generate a new vector pYaliA1-*vio*Dmut following protocols as described in the section "Site-Directed Mutation and Plasmid Construction". Subsequently, the five genes from the violacein pathway were individually assembled into vector backbones containing promoters TEF, ICL1, and ZWF1 YaliBrick cloning protocol,[39,40] generating plasmids pYaliA1-*vio*A, pYaliA1-*vio*B, pYaliA1-*vio*C, pYaliA1-*vio*Dmut, pYaliA1-*vio*E, pYaliH1-*vio*A, pYaliH1-*vio*B, pYaliH1-*vio*C, pYaliH1-*vio*Dmut, pYaliH1-*vio*E, pYaliK1-*vio*A, pYaliK1-*vio*B, pYaliK1-*vio*C, pYaliK1-*vio*Dmut, and pYaliK1-*vio*E, respectively (Figure 2A). Then 15 open reading frames (ORFs) consisting of three promoters, five protein coding sequences, and the XPR2 terminators were PCR amplified (linker used will be discussed later). The resulting fragments (pTEF-*vio*A#, pTEF-*vio*B#, pTEF-*vio*C#, pTEF-*vio*Dmut#, pTEF-*vio*E#, pICL1-*vio*A#, pICL1-*vio*B#, pICL1-*vio*C#, pICL1-*vio*Dmut#, pICL1-*vio*E#, pZWF1-*vio*A#, pZWF1-*vio*B#, pZWF1-*vio*C#, pZWF1-*vio*Dmut#, and pZWF1-*vio*E#) will be used as modular parts in the subsequent Golden Gate assembly (Figure 2B).

Linker Optimization. Exonuclease-based homology recombination methods, such as Gibson assembly, require a 20–40 bp overlapping sequence at the terminus of the DNA fragments to specify the assembly order.[41] One limitation is that DNA fragments with sequence homology at the ends

https://dx.doi.org/10.1021/acssynbio.0c00469
ACS Synth. Biol. 2021, 10, 115–124

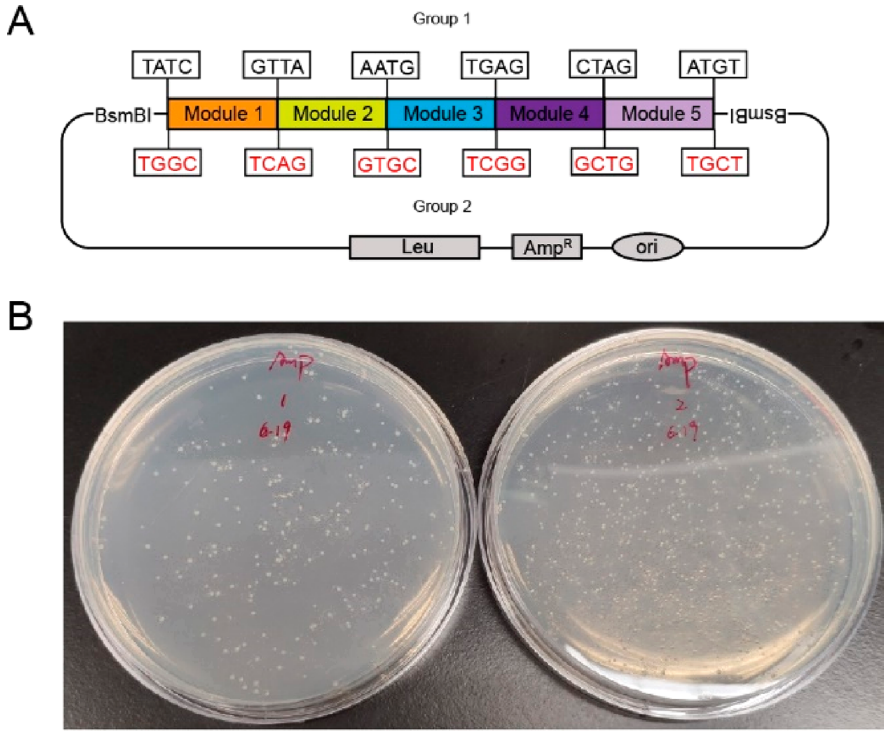

Figure 3. Two groups of linkers used in Golden Gate assembly (A). Transformation efficiency as an indicator of pathway assembly efficiency (B).

cannot be assembled using this method. This limitation can be easily resolved through ePathBrick[32] or Golden Gate assembly. Unlike BioBrick-based cloning, Golden Gate assembly, relying on the type IIs restriction enzymes, has a number of advantages over the traditional restriction endonuclease cloning and BioBrick methods.[42] These type IIs enzymes cut outside of their recognition sequence, forming 4-bp sticky overhangs that can be easily customized to guide the assembly order of any synthetic DNA fragments.[42,43] If designed properly, these type IIs recognition sites will not be retained in the final construct, which allows for efficient and combinatorial cloning without the presence of digestion scars. Therefore, the selection of the 4-bp linkers or adapters in the Golden Gate method is critical to the accuracy and efficiency of the assembly.[33,44] Since all the five modular parts in the violacein pathway are complete ORFs, the linkers that are placed upstream of the promoters or downstream of the terminators will have minimal effect on the ORF transcription and translation. Therefore, the only constraints to design and select the linkers are unique and nonpalindromic to ensure effective cloning. Theoretically, the 4-bp linker may have 4^4 (256) different combinations, here we only need to choose six unique linkers that direct the assembly of the five gene fragments and the vector backbone.

In this work, we chose two sets of end linkers, the first group is TATC, GTTA, AATG, TGAG, CTAG, ATGT and the second group is TGGC, TCAG, GTGC, TCGG, GCTG, TGCT that are recommended from HamediRad's list[33] (Figure 3). Five fragments (pTEF-vioA#, pTEF-vioB#, pTEF-vioC#, pTEF-vioDmut#, and pTEF-vioE#) and the vector pYaliGG were used to test the efficiency of these linkers. These two reactions were performed in parallel under the same reaction conditions. For example, we kept the Golden Gate assembly steps and the concentration of each Golden Gate modular parts exactly the same. After ligation, 1 μL of the assembly reaction from each tube was used for electroporation into *E. coli* NEB5α, respectively, and 1 μL of outgrowth was spread onto selective LB agar plates containing ampicillin. As shown in Figure 3B, the number of colonies on plate 2 (using group 2 linker) was significantly higher than the number of colonies on plate 1 (using group 1 linker). As such, the group 2 linker was selected for subsequent library construction.

Library Construction and Screening. For a five-gene biosynthetic pathway with three varying promoter strengths, we could construct a violacein pathway library containing 243 (3^5) variants with the 15 Golden Gate modular parts that were prepared by using our optimal linkers. The plasmid pYaliGG, which was derived from pYaliXP free of the BsmBI digestion site (Figure S1), was used as the vector backbone to direct all the modular parts to assemble in the right order. After Golden Gate assembly, the reaction was transformed into *E. coli* DH5α. Then the *E. coli* recombinant strains were cultivated, and the mixture of plasmids containing all the assembled pathways was prepared and transformed into *Y. lipolytica* Po1g (Leu−). The recombinant yeast colonies were screened on the agar plates with CSM-Leu minimal media. Since the violacein pathway may generate a number of distinct pigments,[45] after 3 days incubation at 30 °C, the single colonies on the plate may contain three colorful pigments: violacein (purple), deoxyviolacein (pink), and proviolacein (green). Through the spectrophotometric reading of the extracted solution in the liquid culture, we were able to roughly quantify the production of violacein and deoxyviolacein from each colony (Figure 4). The quantification of proviolacien (green product) is not possible in this study, due to the lack of the proviolacein standards.

The initial screening of 20 colonies (8.2% of the library coverage) revealed a significant difference in violacein titer, which demonstrated the importance of accurately regulating the transcriptional strength of each gene in the violacein

https://dx.doi.org/10.1021/acssynbio.0c00469
ACS Synth. Biol. 2021, 10, 115−124

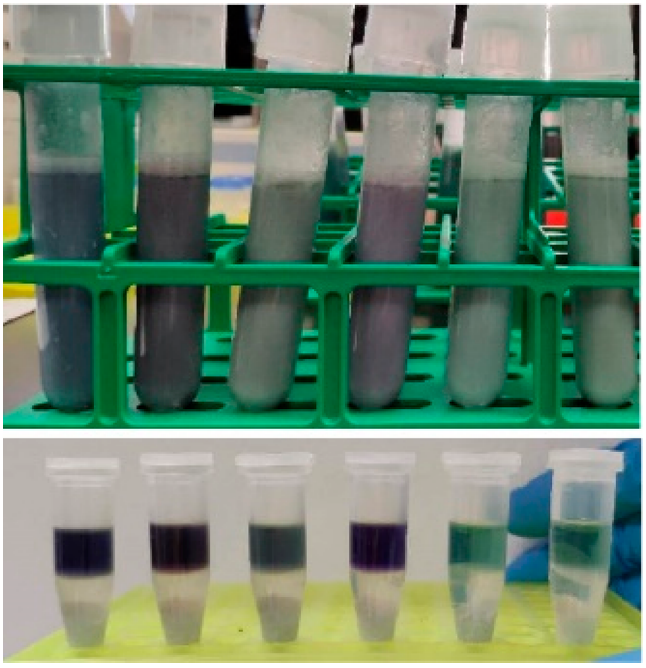

Figure 4. Violacein pathway library transformed into *Y. lipolytica* yields three colorful compounds: green (proviolacein), purple (violacein), and deoxyviolacein (pink). The intensity of the pinkness indicates the percentage of the deoxyviolacein in the culture.

pathway (Figure 5). The highest violacein yield obtained from our library reaches 34.77 mg/L, which is 51 times higher than the yield of the lowest-yielding producer (0.68 mg/L). All the plasmids in the pathway library were then sequenced to determine the sequence of the promoter used for each gene in the pathway. After analyzing the sequencing data, we concluded that the highest violacein titers were obtained when all the five genes were controlled by the strongest TEF promoter (Figure 5). On the other hand, the highest deoxyviolacien titer was obtained when the *vio*B, *vio*D, and *vio*E genes were controlled by the weakest ZWF1 promoter (Figure 5). It is likely that the expression of *vio*D gene controls the production of the byproduct deoxyvioalcein. Violacein production was generally decreased as the transcriptional strength of the promoters were shifted from strong to weak activity (Figure 5).

Because of the bifunctional enzyme *vio*C, deoxyviolacein is produced as the major byproduct of the violacein pathway in the wild strains. Deoxyviolacein is structurally identical to that of violacein, except for the missing oxygen atom at the six position of the indole ring (Figure 1). Violacein produced by the wild strains was usually mixed with up to 10% deoxyviolacein,[46,47] but when the expression of *vio*D was regulated by the weakest promoter ZWF1, the production ratio of violacein and deoxyviolacein was significantly reversed. For example, the proportion of deoxyviolacein in the total products reaches up to 91.34% (the promoter sequence for the five genes *vio*ABCDE is TEF-ZWF1-TEF-ZWF1-ZWF1) (Figure 5). This result is consistent with that of previous work, that the

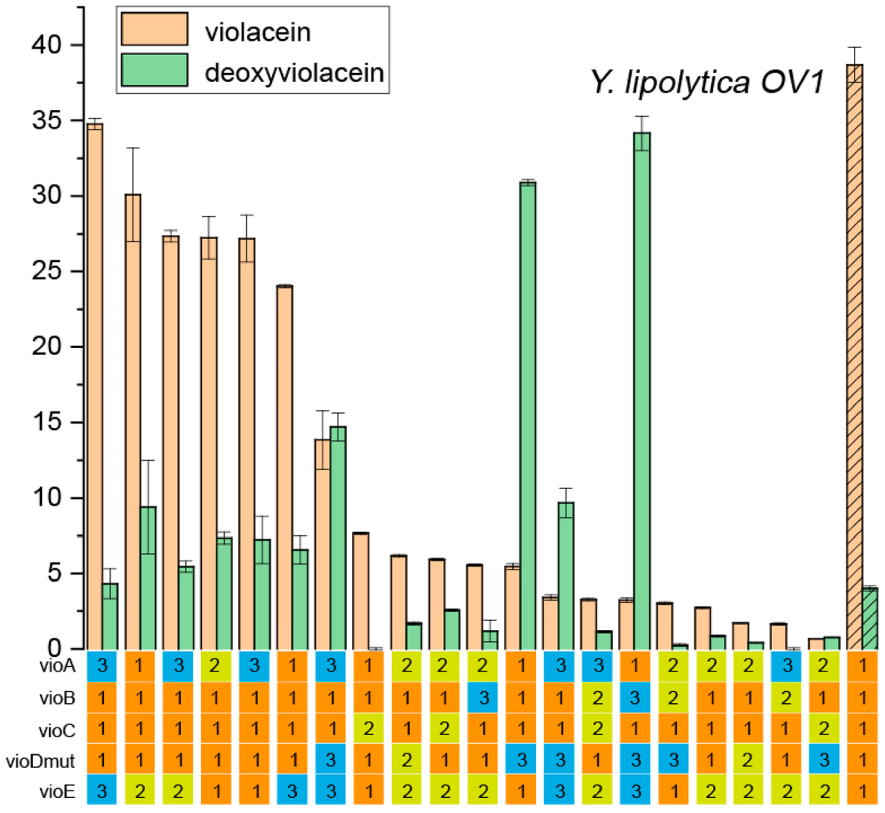

Figure 5. Screening of violacein production (mg/L) from randomized promoter library. Mutants tested in this study cover about 8.5% of the total library size (20/243). Sequence analysis of the library is shown below the horizontal axis. The three endogenous promoters of *Y. lipolytica* were assigned numbers and colors from strong to weak promoter strength as interpreted as TEF promoter, 1, orange; ICL1 promoter, 2, green; ZWF1 promoter, 3, blue.

https://dx.doi.org/10.1021/acssynbio.0c00469
ACS Synth. Biol. 2021, 10, 115−124

expression strength of *vio*D will significantly affect the production of deoxyviolacein. When the *vio*D gene is completely missing or knocked out, even pure deoxyviolacein can be obtained.[48]

We believe that the relative promoter strength of VioA and VioE determines the amount of deoxyviolacein produced in this system. When VioE was under the control of the medium strength ICL promoter (strain #2 in Figure 5), the strain produces more byproduct, deoxyviolacein, than the case when VioE was under the control of the weak promoter ZWF1 (strain #1 in Figure 5). On the other hand, strain #1 (VioA on weak promoter) produced more violacein than strain #2 (VioA on strong promoter), indicating that the relative promoter strength of VioA did not play a significant role in determining the final violacein titer. If we checked across the violacein and deoxyviolacein titer in our strain library (Figure 5), we can conclude that strong expression of VioC benefits both violacein and deoxyviolacein production, and strong expression of VioB and VioD also benefits violacein production. However, high deoxyviolacein production was only associated with the weak expression of VioD (Figure 5). These data reveal the complicated metabolic activity of the branched metabolic pathway when the same biosynthetic gene (VioC) was shared between the byproduct pathway and the target pathway.

Pathway and Fermentation Conditions Optimization for Increased Violacein Production. Since genes regulated by strong TEF promoters are advantageous to violacein production, to further increase the yield, we constructed the strain so that all five genes were regulated by a TEF promoter, generating the strain *Y. lipolytica* OV1. This strain produced 38.68 mg/L violacein, and the proportion of deoxyviolacein is also within a reasonable range (9.41% of the total violacein, Figure 5), demonstrating that strong gene expression for all five genes is indeed critical to improve the violacein production in *Y. lipolytica*.

The carbon to nitrogen ratio plays a major role in regulating the metabolic activity of lipogenic pathways in *Y. lipolytica*.[49] To understand whether the C/N ratio affects vaiolacein production, we tested the violacein production of the top producing strain *Y. lipolytica* OV1 cultivated in CSM-Leu with a C/N ratio of 60, 80, 100, and 120, respectively. Since the maximum absorption wavelength of violacein (570 nm) is close to the detection wavelength of the OD_{600}, to avoid optical interference, dry cell weight instead of OD_{600} was used to quantify cell growth. As shown in Figure 6, the dry cell weight increased substantially as we increased the C/N ratio. However, violacein production remained nearly constant from 38 mg/L to 41 mg/L, and the same trend was observed in the production of deoxyviolacein, regardless of the C/N variations (Figure 6). Since the yield is slightly increased under the condition of a C/N ratio of 60, the subsequent experiment will be carried out under the condition of a C/N ratio of 60.

pH has played a critical role in regulating cell physiology and metabolic activity. Low pH has been routinely observed in *Y. lipolytica* culture due to the accumulation of organic acids.[50] To evaluate the effects of pH on cell growth and violacein production, the cultivation pH was adjusted by adding 10 g/L $CaCO_3$, or by buffering with NaH_2PO_4 and Na_2HPO_4 to pH 6.0, 6.5, 7.0, and 7.5, with initial unbuffered media as control (pH 4.5). As shown in Figure 7, media pH strongly influences cell growth (data of samples adding 10 g/L $CaCO_3$ was not shown, due to insoluble $CaCO_3$ crystals interfering with dry cell weight). Surprisingly, the yeast grew better under mild

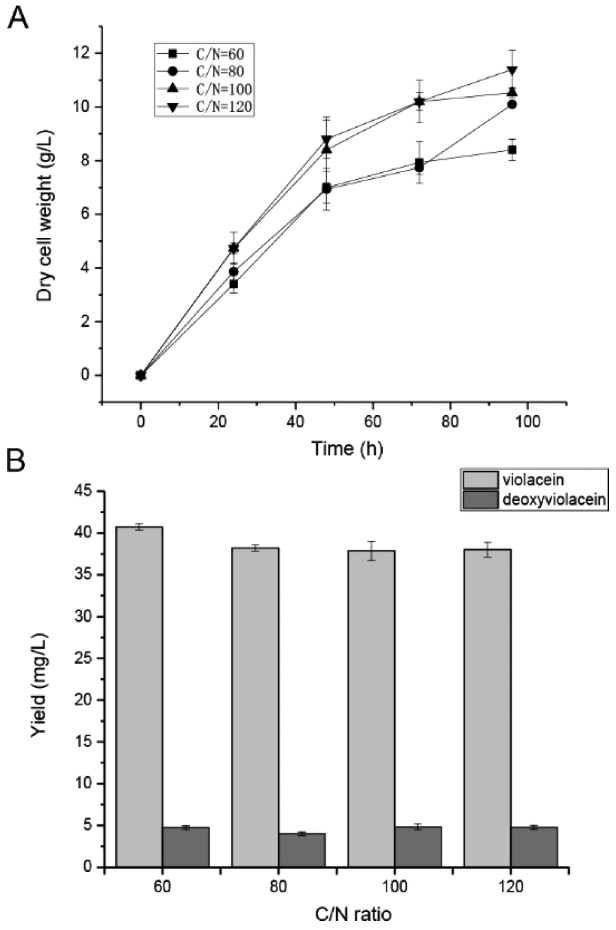

Figure 6. Cell growth (A) and violacein and deoxyviolacein yield (B) in shake flask fermentation by strain *Y. lipolytica* OV1 with different C/N ratios, cultivated in CSM-leu medium at 30 °C. Violacein and deoxyviolacein were quantified by HPLC, with triplicate samples.

acidic or alkaline conditions. For example, when the initial pH is 7.5 or 4.5, the cell growth rate is the fastest, and the dry cell weight reaches 11.13 g/L and 9.54 g/L at 120 h, respectively. However, when the media pH was maintained at 6.0, 6.5, and 7.0, the cell growth noticeably slowed down, and the dry cell weight was only 7.73, 4.07, and 4.50 g/L, respectively.

Despite the fact that cell growth was rapid under pH 7.5, violacein production did not increase accordingly (Figure 7). As the media pH was buffered from 6.0 to 7.0, violacein production decreased gradually (Figure 7), possibly due to the acidophilic nature of the violacein pathway. Most strikingly, $CaCO_3$ was found to be a superior supplement to buffer media pH. The carbonate group (CO_3^{2-}) will effectively neutralize the organic acids accumulated during the fermentation. At the end of the fermentation, 70.04 mg/L violacein and 5.28 mg/L deoxyviolacein were produced from the yeast culture supplemented with $CaCO_3$. Because of the inexpensive nature of $CaCO_3$, this result also indicated that $CaCO_3$ was the preferred buffer to adjust media pH for yeast fermentation.

CONCLUSIONS

In this work, the optimization of 4-bp linkers of the Golden Gate assembly allows us to quickly build violacein biosynthetic pathway libraries with varying promoter strengths in *Y. lipolytica* and access three colorful compounds (green, purple, and pink). After optimizing the cultivation conditions,

https://dx.doi.org/10.1021/acssynbio.0c00469
ACS Synth. Biol. 2021, 10, 115−124

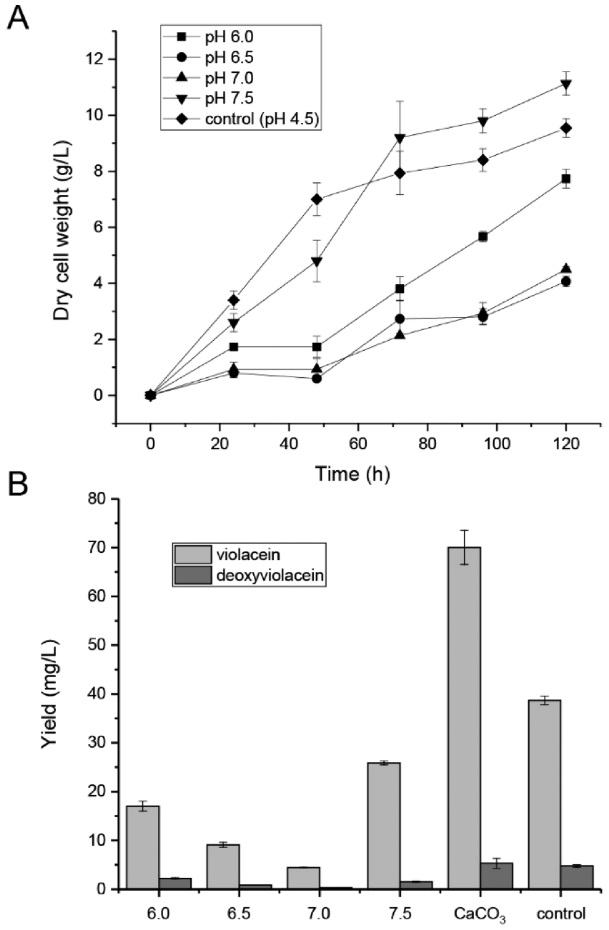

Figure 7. Cell growth (A) and violacein and deoxyviolacein yield (B) in shake flask fermentation by strain *Y. lipolytica* OV1 with pH 6.0, 6.5, 7.0, 7.5, $CaCO_3$ and the control (pH 4.5), cultivated in CSM-leu medium at 30 °C. Violacein and deoxyviolacein were quantified by HPLC, with triplicate samples.

violacein production was increased by 84.2%, reaching to 70.04 mg/L when the C/N ratio was controlled at 60 and the media was buffered with $CaCO_3$. This work provided a hands-on protocol for us to build pathway libraries with varying promoter strengths that maximize the output of a predefined biosynthetic pathway.

MATERIALS AND METHODS

Strains, Plasmids, Primers, and Culture Conditions. The bacterial strains, plasmids, and primers used in this study are listed in the Supporting Information, Table S1. *Escherichia coli* NEB5α high efficiency competent cells were obtained from NEB (New England Biolabs Ipswich, MA). The auxotrophic *Y. lipolytica* Po1g (Leu−) was purchased from Yeastern Biotech Company (Taipei, Taiwan). *Y. lipolytica* XP1 harboring the plasmid pYaliA1-vioDCBAE was stored in our lab.[39] YPD medium contains 20 g/L glucose (Sigma-Aldrich), 10 g/L yeast extract (Sigma-Aldrich), and 20 g/L peptone (Sigma-Aldrich). YNB medium (C/N = 60, 80, 100, 120) contains 1.7 g/L yeast nitrogen base (without amino acids and ammonium sulfate) (Difco), 1.1 g/L ammonium sulfate (Sigma-Aldrich), 0.69 g/L CSM-Leu (Sunrise Science Products, Inc.), and 30, 40, 50, 60 g/L glucose, respectively. YNB medium (pH 6.0, 6.5, 7.0, 7.5) contains 1.7 g/L yeast nitrogen base (without amino acids and ammonium sulfate) (Difco), 1.1 g/L ammonium sulfate (Sigma-Aldrich), 0.69 g/L CSM-Leu (Sunrise Science Products, Inc.), 30 g/L glucose, and was adjusted to pH 6.0, 6.5, 7.0, 7.5, respectively, through Na_2HPO_4 and NaH_2PO_4. YNB medium with $CaCO_3$ was made with YNB media supplemented with 10 g/L $CaCO_3$. Selective YNB plates were made with YNB media supplemented with 20 g/L Bacto agar (Difco).

Site-Directed Mutation and Plasmid Construction. All the primers and plasmids used in this study are listed in Table S1. Plasmid extraction, agarose gel electrophoresis, and other DNA manipulations were carried out by using standard protocols.[51] All the plasmids constructed were verified by sequencing.

The pYaliGG vector was constructed on the basis of plasmid pYaliXP. Primers GGmut-S1 and GGmut-A1 were used to amplify fragment GGmut1#, primers GGmut-S2 and GGmut-A2 were used to amplify fragment GGmut2#. Plasmid pYaliXP was enzyme digested via the *Nhe*I and *Bgl*II site, generating fragment pYaliXP#. Then these three fragments were mixed and assembled following the Gibson assembly protocol, generating plasmid pYaliGG. The *vio*D site-directed mutation plasmid pYaliA1-*vio*Dmut was constructed on the basis of plasmid pYaliA1-*vio*D. Primers D1-mut-s1 and D1-mut-a1 were used to amplify fragment D1mut1#; primers D1-mut-s2 and D1-mut-a2 were used to amplify fragment D1mut2#. Plasmid pYaliA1-vioD were enzyme digested via the *Cla*I and *Kpn*2I site, generating fragment pYaliA1#. Then these three fragments were mixed and assembled following the Gibson assembly protocol, generating plasmid pYaliA1-vioDmut (Figure S1).

The coding sequences of *vio*A, *vio*B, *vio*C, *vio*Dmut, and *vio*E were assembled into pYaliH1 and pYaliK1 vector backbones, respectively, from plasmid pYaliA1-*vio*A, pYaliA1-*vio*B, pYaliA1-*vio*C, pYaliA1-*vio*Dmut, and pYaliA1-*vio*E by restriction enzyme digestion via the *Xba*I and *Kpn*I site, resulting plasmids pYaliH1-*vio*A, pYaliH1-*vio*B, pYaliH1-*vio*C, pYaliH1-*vio*Dmut, pYaliH1-*vio*E, pYaliK1-*vio*A, pYaliK1-*vio*B, pYaliK1-*vio*C, pYaliK1-*vio*Dmut, and pYaliK1-*vio*E, respectively.

***Y. lipolytica* Transformation Procedures.** The *Y. lipolytica* competent cell preparation and transformation procedures were carried out by using previously reported procedures.[52] In brief, a single colony from plates was inoculated into 10 mL of YPD medium in a 50 mL shake flask. The cells were allowed to grow overnight (16−24 h) with shaking; 500 μL of cells was harvested from the above culture and washed twice with 1 mL of ddH_2O. After that, cells were resuspended in 100 μL of transformation buffer (including 90 μL of 50% PEG4000, 5 μL of 2 M lithium acetate, and 5 μL of boiled single strand DNA (salmon sperm, denatured) with 5 μL of DNA products (200−500 ng plasmids or DNA fragments). The transformation mixtures were incubated at 30 °C for 30−45 min and then vortexed for 10 s every 10 min. They then underwent and additional 10 min heat shock at 39 °C to increase transformation efficiency and were spread on selected plates with auxotroph.

Golden Gate Cloning. Fragments used in Golden Gate assembly were PCR amplified. All the primers and plasmids used in this assembly are listed in Table S1. Golden Gate plasmids were assembled in the presence of 30 U BsmBI (New England Biolabs Ipswich, MA), 1000 U T4 DNA ligase (New England Biolabs Ipswich, MA), 2 μL of NEBuffer 3.1 (New England Biolabs Ipswich, MA), and 1 mM ATP (New England Biolabs Ipswich, MA). All the fragments to be assembled were

https://dx.doi.org/10.1021/acssynbio.0c00469
ACS Synth. Biol. 2021, 10, 115−124

purified and used in equimolar ratios at a final concentration of 20 pmol, then the volume was increased to 25 μL with ddH_2O. The assembly was transferred to a thermocycler which was programed as follows: (5 min at 37 °C, 5 min at 16 °C) × 30 cycles followed by 5 min at 60 °C, then transformed into *E. coli* NEB5α or *Y. lipolytica* Po1g (Leu−).

Seed Culture and Fermentation Procedure. For preparing seed inocula, strains were cultivated into 50 mL of CSM-Leu medium containing 20 g/L glucose, 5 g/L ammonium sulfate (Sigma-Aldrich), 0.69 g/L CSM-Leu (Sunrise Science Products, Inc.), and 1.7 g/L yeast nitrogen base (without amino acids and ammonium sulfate) (Difco) in 250 mL shake flasks for 24 h with agitation at 250 rpm at 30 °C. For the C/N ratio and pH optimization in a shake flask, 5% (v/v) of the seed culture was inoculated to the corresponding medium, with different C/N ratios, pH values, and $CaCO_3$ concentrations. All the strains were cultured at 250 rpm, 30 °C up to 120 h for violacein production.

Analytical Methods. A violacein standard was purchased from Sigma-Aldrich and was dissolved in methanol. The maximum absorption wavelength of violacein was determined through full wavelength scanning from 230 to 750 nm by a microplate reader (Synergy H1 Hybrid Multi-Mode Microplate Reader, BioTek, Winooski, VT) (Figure S2).

A standard curve for violacein was prepared by diluting the standard (Sigma-Aldrich) with methanol into concentrations of 10, 20, 30, 40, 50, 60, 70, 80, 90, and 100 mg/L. The analysis of violacein was performed by high-performance liquid chromatography (HPLC) (Agilent Technologies 1220 Infinity II LC, USA) using Agilent Eclipse Plus C18 column (4.6 mm × 100 mm, 3.5 μm, USA), equipped with UV detector at 570 nm. Mobile phase A was H_2O with 0.1% acetate acid, and mobile phase B was methanol with 0.1% acetate acid. A stepwise gradient elution at a flow rate of 0.4 mL/min was used, following the gradient profiles as follows: ramping from 100% to 20% A in 0∼5 min, maintaining 20% A (80% B) in 5∼8 min, ramping from 20% to 100% A in 8∼12 min, and maintaining100% A in 12∼15 min. The deoxyviolacein standard was diluted with methanol into concentrations at 0.6, 1, 1.8, 2.5, 3, 3.5, and 4 mg/L, and was analyzed by HPLC with the same method of violacein. A spectrophotometer-based standard curve was also developed through a microplate reader at 570 nm. The violacein standard was diluted with ethanol at the concentrations of 2, 4, 6, 8, 10 mg/L.

The biomass was measured as dry cell weight. A 500 μL sampling of yeast cells was harvested and centrifuged in a microcentrifuge tube at 13 000 rpm for 5 min. The upper broth was discarded, and the cell pellet was washed twice with ddH_2O, and then dried in an oven at 60 °C until the weight did not change. The difference in the weight of microcentrifuge tube with and without cells was then calculated.

■ ASSOCIATED CONTENT

Supporting Information

The Supporting Information is available free of charge at https://pubs.acs.org/doi/10.1021/acssynbio.0c00469.

> Bacterial strains, plasmids, and primers used in this work; site-directed mutation site of pYaliA1-*vio*Dmut and pYaliGG; UV−visible absorption spectrum of violacein standards (PDF)

■ AUTHOR INFORMATION

Corresponding Authors

Liang Zhang − *School of Biotechnology, Jiangnan University, Wuxi 214122, China*; Phone: +1(410)-455-2474; Email: zhangl@jiangnan.edu.cn; Fax: +1(410)-455-1049

Peng Xu − *Chemical, Biochemical and Environmental Engineering, University of Maryland Baltimore County, Baltimore, Maryland 21250, United States*; orcid.org/0000-0002-0999-8546; Email: pengxu@umbc.edu

Authors

Yingjia Tong − *School of Biotechnology, Jiangnan University, Wuxi 214122, China; Chemical, Biochemical and Environmental Engineering, University of Maryland Baltimore County, Baltimore, Maryland 21250, United States*; orcid.org/0000-0003-1025-674X

Jingwen Zhou − *School of Biotechnology, Jiangnan University, Wuxi 214122, China*; orcid.org/0000-0002-3949-3733

Complete contact information is available at: https://pubs.acs.org/10.1021/acssynbio.0c00469

Author Contributions

P.X. conceived and designed the topic. Y.J.T. performed genetic cloning, strain cultivation, fermentation, extraction, analytical assay, and analyzed the data. Y.J.T. and P.X. wrote the manuscript. Y.J.T. was coadvised by J.W.Z. and L.Z.

Notes

The authors declare no competing financial interest.

■ ACKNOWLEDGMENTS

This work was supported by the Cellular & Biochem Engineering Program of the National Science Foundation under Grant No. 1805139 and the Bill & Melinda Gates Foundation under Grant No. OPP1188443. Y.J.T. would like to thank the China Scholarship Council for funding support.

■ REFERENCES

(1) Baricz, A., Teban, A., Chiriac, C. M., Szekeres, E., Farkas, A., Nica, M., Dascalu, A., Oprisan, C., Lavin, P., and Coman, C. (2018) Investigating the potential use of an Antarctic variant of Janthinobacterium lividum for tackling antimicrobial resistance in a One Health approach. *Sci. Rep. 8* (1), 15272.

(2) Kanelli, M., Mandic, M., Kalakona, M., Vasilakos, S., Kekos, D., Nikodinovic-Runic, J., and Topakas, E. (2018) Microbial Production of Violacein and Process Optimization for Dyeing Polyamide Fabrics With Acquired Antimicrobial Properties. *Front. Microbiol. 9*, 1495.

(3) Aruldass, C. A., Masalamany, S. R. L., Venil, C. K., and Ahmad, W. A. (2018) Antibacterial mode of action of violacein from Chromobacterium violaceum UTM5 against Staphylococcus aureus and methicillin-resistant Staphylococcus aureus (MRSA). *Environ. Sci. Pollut. Res. 25* (6), 5164−5180.

(4) Mart'yanov, S. V., Letarov, A. V., Ivanov, P. A., and Plakunov, V. K. (2018) Stimulation of Violacein Biosynthesis in Chromobacterium violaceum Biofilms in the Presence of Dimethyl Sulfoxide. *Microbiology 87* (3), 437−440.

(5) Ahmad, W. A., Yusof, N. Z., Nordin, N., Zakaria, Z. A., and Rezali, M. F. (2012) Production and Characterization of Violacein by Locally Isolated Chromobacterium violaceum Grown in Agricultural Wastes. *Appl. Biochem. Biotechnol. 167* (5), 1220−1234.

(6) Yang, L. H., Xiong, H., Lee, O. O., Qi, S. H., and Qian, P. Y. (2007) Effect of agitation on violacein production in Pseudoalteromonas luteoviolacea isolated from a marine sponge. *Lett. Appl. Microbiol. 44* (6), 625−630.

(7) Batista, A. H. M., Moreira, A. C. D., de Carvalho, R. M., Sales, G. W. P., Nogueira, P. C. N., Grangeiro, T. B., Medeiros, S. C., Silveira,

E. R., and Nogueira, N. A. P. (2017) Antimicrobial Effects of Violacein against Planktonic Cells and Biofilms of Staphylococcus aureus. *Molecules 22* (10), 1534.
(8) Hashimi, S. M., Xu, T., and Wei, M. Q. (2015) Violacein anticancer activity is enhanced under hypoxia. *Oncol. Rep. 33* (4), 1731−1736.
(9) Andrighetti-Frohner, C. R., Antonio, R. V., Creczynski-Pasa, T. B., Barardi, C. R., and Simoes, C. M. (2003) Cytotoxicity and potential antiviral evaluation of violacein produced by Chromobacterium violaceum. *Mem. Inst. Oswaldo Cruz 98* (6), 843−848.
(10) Bilsland, E., Tavella, T. A., Krogh, R., Stokes, J. E., Roberts, A., Ajioka, J., Spring, D. R., Andricopulo, A. D., Costa, F. T. M., and Oliver, S. G. (2018) Antiplasmodial and trypanocidal activity of violacein and deoxyviolacein produced from synthetic operons. *BMC Biotechnol. 18* (1), 22.
(11) Matz, C., Deines, P., Boenigk, J., Arndt, H., Eberl, L., Kjelleberg, S., and Jurgens, K. (2004) Impact of violacein-producing bacteria on survival and feeding of bacterivorous nanoflagellates. *Appl. Environ. Microbiol. 70* (3), 1593−1599.
(12) Pemberton, J. M., Vincent, K. M., and Penfold, R. J. (1991) Cloning and heterologous expression of the violacein biosynthesis gene-cluster from chromobacterium-violaceum. *Curr. Microbiol. 22* (6), 355−358.
(13) Balibar, C. J., and Walsh, C. T. (2006) In vitro biosynthesis of violacein from L-tryptophan by the enzymes VioA-E from Chromobacterium violaceum. *Biochemistry 45* (51), 15444−15457.
(14) Sanchez, C., Brana, A. F., Mendez, C., and Salas, J. A. (2006) Reevaluation of the violacein biosynthetic pathway and its relationship to indolocarbazole biosynthesis. *ChemBioChem 7* (8), 1231−1240.
(15) Fang, M. Y., Zhang, C., Yang, S., Cui, J. Y., Jiang, P. X., Lou, K., Wachi, M., and Xing, X. H. (2015) High crude violacein production from glucose by Escherichia coli engineered with interactive control of tryptophan pathway and violacein biosynthetic pathway. *Microb. Cell Fact. 14* (1), 8.
(16) Immanuel, S. R. C., Banerjee, D., Rajankar, M. P., and Raghunathan, A. (2018) Integrated constraints based analysis of an engineered violacein pathway in Escherichia coli. *BioSystems 171*, 10−19.
(17) Xu, P., Rizzoni, E. A., Sul, S.-Y., and Stephanopoulos, G. (2017) Improving metabolic pathway efficiency by statistical model-based multivariate regulatory metabolic engineering. *ACS Synth. Biol. 6* (1), 148−158.
(18) Czajka, J. J., Nathenson, J. A., Benites, V. T., Baidoo, E. E. K., Cheng, Q., Wang, Y., and Tang, Y. J. (2018) Engineering the oleaginous yeast Yarrowia lipolytica to produce the aroma compound *β*-ionone. *Microb. Cell Fact. 17* (1), 136−136.
(19) Ma, J., Gu, Y., Marsafari, M., and Xu, P. (2020) Synthetic biology, systems biology, and metabolic engineering of Yarrowia lipolytica toward a sustainable biorefinery platform. *J. Ind. Microbiol. Biotechnol. 47* (9−10), 845−862.
(20) Ledesma-Amaro, R., Lazar, Z., Rakicka, M., Guo, Z., Fouchard, F., Coq, A. C., and Nicaud, J. M. (2016) Metabolic engineering of Yarrowia lipolytica to produce chemicals and fuels from xylose. *Metab. Eng. 38*, 115−124.
(21) Robles-Rodríguez, C. E., Muñoz-Tamayo, R., Bideaux, C., Gorret, N., Guillouet, S. E., Molina-Jouve, C., Roux, G., and Aceves-Lara, C. A. (2018) Modeling and optimization of lipid accumulation by Yarrowia lipolytica from glucose under nitrogen depletion conditions. *Biotechnol. Bioeng. 115* (5), 1137−1151.
(22) Sabra, W., Bommareddy, R. R., Maheshwari, G., Papanikolaou, S., and Zeng, A.-P. (2017) Substrates and oxygen dependent citric acid production by Yarrowia lipolytica: insights through transcriptome and fluxome analyses. *Microb. Cell Fact. 16* (1), 78−78.
(23) Li, H., and Alper, H. S. (2016) Enabling xylose utilization in Yarrowia lipolytica for lipid production. *Biotechnol. J. 11* (9), 1230−1240.
(24) Gatter, M., Ottlik, S., Kövesi, Z., Bauer, B., Matthäus, F., and Barth, G. (2016) Three alcohol dehydrogenase genes and one acetyl-CoA synthetase gene are responsible for ethanol utilization in Yarrowia lipolytica. *Fungal Genet. Biol. 95*, 30−38.
(25) Liu, H., Marsafari, M., Wang, F., Deng, L., and Xu, P. (2019) Engineering acetyl-CoA metabolic shortcut for eco-friendly production of polyketides triacetic acid lactone in Yarrowia lipolytica. *Metab. Eng. 56*, 60−68.
(26) Liu, H., Wang, F., Deng, L., and Xu, P. (2020) Genetic and bioprocess engineering to improve squalene production in Yarrowia lipolytica. *Bioresour. Technol. 317*, 123991.
(27) Iwama, R., Kobayashi, S., Ishimaru, C., Ohta, A., Horiuchi, H., and Fukuda, R. (2016) Functional roles and substrate specificities of twelve cytochromes P450 belonging to CYP52 family in n-alkane assimilating yeast Yarrowia lipolytica. *Fungal Genet. Biol. 91*, 43−54.
(28) Sands, B., and Brent, R. (2016) Overview of Post Cohen-Boyer Methods for Single Segment Cloning and for Multisegment DNA Assembly. *Curr. Protoc. Mol. Biol. 113* (1), 1−20.
(29) Xu, P., Bhan, N., and Koffas, M. A. (2013) Engineering plant metabolism into microbes: from systems biology to synthetic biology. *Curr. Opin. Biotechnol. 24* (2), 291−299.
(30) Celinska, E., Ledesma-Amaro, R., Larroude, M., Rossignol, T., Pauthenier, C., and Nicaud, J. M. (2017) Golden Gate Assembly system dedicated to complex pathway manipulation in Yarrowia lipolytica. *Microb. Biotechnol. 10* (2), 450−455.
(31) Fonseca, J. P., Bonny, A. R., Kumar, G. R., Ng, A. H., Town, J., Wu, Q. C., Aslankoohi, E., Chen, S. Y., Dods, G., Harrigan, P., Osimiri, L. C., Kistler, A. L., and El-Samad, H. (2019) A Toolkit for Rapid Modular Construction of Biological Circuits in Mammalian Cells. *ACS Synth. Biol. 8* (11), 2593−2606.
(32) Xu, P., Vansiri, A., Bhan, N., and Koffas, M. (2012) ePathBrick: A Synthetic Biology Platform for Engineering Metabolic Pathways in E-coli. *ACS Synth. Biol. 1* (7), 256−266.
(33) HamediRad, M., Weisberg, S., Chao, R., Lian, J., and Zhao, H. (2019) Highly Efficient Single-Pot Scarless Golden Gate Assembly. *ACS Synth. Biol. 8* (5), 1047−1054.
(34) Egermeier, M., Sauer, M., and Marx, H. (2019) Golden Gate-based metabolic engineering strategy for wild-type strains of Yarrowia lipolytica. *FEMS Microbiol. Lett. 366* (4), fnz022.
(35) Larroude, M., Park, Y. K., Soudier, P., Kubiak, M., Nicaud, J. M., and Rossignol, T. (2019) A modular Golden Gate toolkit for Yarrowia lipolytica synthetic biology. *Microb. Biotechnol. 12* (6), 1249−1259.
(36) Hwang, H. J., Lee, S. Y., and Lee, P. C. (2018) Engineering and application of synthetic nar promoter for fine-tuning the expression of metabolic pathway genes in Escherichia coli. *Biotechnol. Biofuels 11*, 103.
(37) Engler, C., Gruetzner, R., Kandzia, R., and Marillonnet, S. (2009) Golden gate shuffling: a one-pot DNA shuffling method based on type IIs restriction enzymes. *PLoS One 4* (5), e5553.
(38) Lee, J. H., Skowron, P. M., Rutkowska, S. M., Hong, S. S., and Kim, S. C. (1996) Sequential amplification of cloned DNA as tandem multimers using class-IIS restriction enzymes. *Genet. Anal.: Tech. Appl. 13* (6), 139−145.
(39) Wong, L., Engel, J., Jin, E., Holdridge, B., and Xu, P. (2017) YaliBricks, a versatile genetic toolkit for streamlined and rapid pathway engineering in Yarrowia lipolytica. *Metab. Eng. Commun. 5*, 68−77.
(40) Wong, L., Holdridge, B., Engel, J., and Xu, P. (2019) Genetic Tools for Streamlined and Accelerated Pathway Engineering in Yarrowia lipolytica. *Methods Mol. Biol. 1927*, 155−177.
(41) Gibson, D. G., Young, L., Chuang, R. Y., Venter, J. C., Hutchison, C. A., 3rd, and Smith, H. O. (2009) Enzymatic assembly of DNA molecules up to several hundred kilobases. *Nat. Methods 6* (5), 343−345.
(42) Engler, C., and Marillonnet, S. (2014) Golden Gate cloning. *Methods Mol. Biol. 1116*, 119−131.
(43) Marillonnet, S., and Werner, S. (2015) Assembly of Multigene Constructs Using Golden Gate Cloning. *Methods Mol. Biol. 1321*, 269−284.

https://dx.doi.org/10.1021/acssynbio.0c00469
ACS Synth. Biol. 2021, 10, 115−124

(44) Andreou, A. I., and Nakayama, N. (2018) Mobius Assembly: A versatile Golden-Gate framework towards universal DNA assembly. *PLoS One 13* (1), e0189892−e0189892.
(45) Sigurdson, G. T., Tang, P., and Giusti, M. M. (2017) Natural Colorants: Food Colorants from Natural Sources. *Annu. Rev. Food Sci. Technol. 8*, 261−280.
(46) Jiang, P. X., Wang, H. S., Zhang, C., Lou, K., and Xing, X. H. (2010) Reconstruction of the violacein biosynthetic pathway from Duganella sp. B2 in different heterologous hosts. *Appl. Microbiol. Biotechnol. 86* (4), 1077−1088.
(47) Wang, H., Wang, F., Zhu, X., Yan, Y., Yu, X., Jiang, P., and Xing, X.-H. (2012) Biosynthesis and characterization of violacein, deoxyviolacein and oxyviolacein in heterologous host, and their antimicrobial activities. *Biochem. Eng. J. 67*, 148−155.
(48) Jiang, P. X., Wang, H. S., Xiao, S., Fang, M. Y., Zhang, R. P., He, S. Y., Lou, K., and Xing, X. H. (2012) Pathway redesign for deoxyviolacein biosynthesis in Citrobacter freundii and characterization of this pigment. *Appl. Microbiol. Biotechnol. 94* (6), 1521−1532.
(49) Liu, H., Marsafari, M., Deng, L., and Xu, P. (2019) Understanding lipogenesis by dynamically profiling transcriptional activity of lipogenic promoters in Yarrowia lipolytica. *Appl. Microbiol. Biotechnol. 103* (7), 3167−3179.
(50) Lv, Y., Marsafari, M., Koffas, M., Zhou, J., and Xu, P. (2019) Optimizing Oleaginous Yeast Cell Factories for Flavonoids and Hydroxylated Flavonoids Biosynthesis. *ACS Synth. Biol. 8* (11), 2514−2523.
(51) Tong, Y., Ji, X., Shen, M., Liu, L., Nie, Z., and Huang, H. (2016) Constructing a synthetic constitutive metabolic pathway in Escherichia coli for (R, R)-2,3-butanediol production. *Appl. Microbiol. Biotechnol. 100* (2), 637−647.
(52) Gietz, R. D. (2014) Yeast transformation by the LiAc/SS carrier DNA/PEG method. *Methods Mol. Biol. 1163*, 33−44.

https://dx.doi.org/10.1021/acssynbio.0c00469
ACS Synth. Biol. 2021, 10, 115−124